

# Mpemba Effect and Superuniversality across Orders of Magnetic Phase Transition

Sohini Chatterjee,<sup>1</sup> Soumik Ghosh,<sup>1</sup> Nalina Vadakkayil,<sup>1,2</sup> Tanay Paul,<sup>1</sup> Sanat K. Singha,<sup>1,3</sup> and Subir K. Das<sup>1,\*</sup>

<sup>1</sup>*Theoretical Sciences Unit and School of Advanced Materials,*

*Jawaharlal Nehru Centre for Advanced Scientific Research, Jakkur P.O., Bangalore 560064, India*

<sup>2</sup>*Complex Systems and Statistical Mechanics, Department of Physics and Materials Science,*

*University of Luxembourg, Luxembourg, L-1511, Luxembourg*

<sup>3</sup>*Assam Energy Institute, A Centre of Rajiv Gandhi Institute of Petroleum Technology, Sivasagar 785697, India*

(Dated: September 8, 2023)

The quicker freezing of hotter water, than a colder sample, when quenched to a common lower temperature, is referred to as the Mpemba effect (ME). While this counter-intuitive fact remains a surprise since long, efforts have begun to identify similar effect in other systems. Here we investigate the ME in a rather general context concerning magnetic phase transitions. From Monte Carlo simulations of model systems, viz., the  $q$ -state Potts model and the Ising model, with varying range of interaction and space dimension, we assert that hotter paramagnets undergo ferromagnetic ordering faster than the colder ones. The above conclusion we have arrived at following the analyses of the simulation results on decay of energy and growth in ordering following quenches from different starting temperatures, to fixed final temperatures below the Curie points. We have obtained a unique scaling picture, on the strength of the effect, with respect to the variation in spatial correlation in the initial states. These results are valid irrespective of the order of transition and relevant to the understanding of ME in other systems, including water.

## I. INTRODUCTION

If two bodies of liquid water, differing in temperature, are placed in contact with a thermal reservoir, operating at a subzero temperature ( $< 0^\circ\text{C}$ ), the most common prediction will be that the colder between the two will freeze faster. The report in Ref. [1], by Mpemba and Osborne, however, contradicts such an expectation. There has been a surge [1–29] in interest in further investigating this forgotten counter-intuitive fact, which found mention even in the works of Aristotle [30], now referred to as the Mpemba effect (ME). In recent times, questions relevant to the ME are posed in

---

\* [das@jncasr.ac.in](mailto:das@jncasr.ac.in)

more general ways [2], going much beyond the domain of water [1–11]: When two samples of the same material, from two different temperatures, are quenched to a common lower temperature, which one will reach the new equilibrium quicker? If there exists a point of phase transition, between the initial and the final temperatures, for which starting temperature the transformation will occur earlier? There is a rapid growth in interest in studying systems of different types. Experimental studies on systems such as colloidal systems [10], clathrate hydrates [11], carbon nanotube resonators [12] and magnetic alloys [13] show the presence of ME. In the theoretical and computational literature, the varieties that are studied include granular matter [14–17], spin glass [18] and few other systems of magnetic origin [19–22]. Nevertheless, the underlying reason remains a puzzle, inviting the need for stronger theoretical intervention. The pertaining new questions are fundamental from statistical mechanical and other theoretical points of view. In addition, the effect can be exploited to much practical advantages [28].

In the case of water, for a transformation from liquid to solid, overcoming metastability is a serious problem [31]. Nucleation there, as well as in general, is strongly influenced by the choice of the final temperature ( $T_f$ ), the type and the volume fraction of impurity, etc. However, how the role of the starting temperature ( $T_s$ ) enters the picture is an important new fundamental issue. Is it that the above mentioned metastable aspect gets affected by the nature of the initial thermodynamic state in an unexpected order? With in-built frustration in the model Hamiltonian, some of the theoretical works perhaps set the objective of exploring this angle. Such studies are by primarily involving the magnetic systems with anti-ferromagnetic interactions, including spin glasses. However, simpler systems must also be considered. If the effect is found to be present in their evolution dynamics, route to a proper understanding can be easier.

In fact, the standard ferromagnetic Ising model, without any impurity, is seen to exhibit the effect [21]. The positive observation of the ME there was attributed to the structural changes associated with the critical divergence of the spatial correlation with the variation of  $T_s$  in the paramagnetic phase [2, 21]. To justify the validity of the attribution and estimate the corresponding quantitative influence, it is important to study the model in other situations like in different space dimensions ( $d$ ) and with varying range of interactions. Very importantly, it should be checked what are the effects of the order of transitions [2, 22, 29]. This is by considering the fact that in the case of water, the transition is of first order character, while for the Ising model the problem was designed [21] in such a way that the influence of second order transition is captured. Keeping these in mind [2, 22, 29], here we chose the  $q$ -state Potts model [32, 33] for which the order of transition changes with the variation of its number of states  $q$ . Interestingly, we observe the presence of the ME in all the above mentioned cases. For the Potts model, it appears that with the

increase of  $q$  the effect gets weaker, as far as the variation in  $T_s$  is concerned. However, interestingly, regarding the effects of spatial correlation in the initial states there exists a unique scaling, not only for the simple variation of  $q$ , but also with the change of the order of transition and space dimension. We believe, in addition to being important for the class of systems considered, this study also provides crucial angle with respect to the interpretation of the effect in water.

## II. MODELS AND METHODS

As already mentioned, here we study a class of discrete spin systems with pure ferromagnetic interactions. We investigate the Ising model [32] in different dimensions, having short and long-range inter-site potentials [34]. Furthermore, generalization of this two-component system into multi-component ones have also been considered. In general, the Hamiltonian can be written as  $H = -\sum_{i(\neq)j} J(r_{ij})\delta_{S_i, S_j}$ ;  $S_i, S_j = 1, 2, \dots, q$ ;  $r_{ij}$  being the separation between lattice sites. For  $q = 2$ , this Potts model Hamiltonian corresponds to the Ising model, differing only by a factor of 2. The latter, by correcting for the factor, we have studied in  $d = 2$  and 3, with nearest neighbor (NN) interactions, by setting the interaction strength  $J$  to unity, on square and simple cubic lattices, respectively. In  $d = 2$ , we have also presented results for the long-range (LR) version of the Ising model with [34]  $J(r_{ij}) = 1/r_{ij}^{2+\sigma}$ , for  $\sigma = 0.8$ , again using the square lattice. Most extensive results are obtained for the (short-range) Potts model,  $q$  varying between 2 and 10. The critical temperature for this model has the  $q$ -dependence [32]  $T_c = J/[k_B \ln(1 + \sqrt{q})]$ ,  $k_B$  being the Boltzmann constant, to be set to unity. Depending on the value of  $q$  the order of transition can alter. For  $q > 4$  the model loses its ‘‘critical’’ character [33], the transition being of first order. For the Ising case, the values of  $T_c$  in  $d = 2$  and 3 are  $\simeq 2.269 J/k_B$  and  $\simeq 4.51 J/k_B$ , respectively [32]. For the long-range case we have used [35]  $T_c = 9.765 J/k_B$ .

The kinetics of transition from para to ferro states are studied via Monte Carlo simulations [32], with the Glauber spin-turn mechanism [32]. The preparation of the initial configurations near the critical point encounters critical slowing down [32]. To avoid this, we have used cluster algorithms. In the case of Ising or Potts model, this is done by implementing the Wolff algorithm [36], and for the LR Ising model, we have used the Fukui-Todo algorithm [35, 37]. The presence of the correlated spatial fluctuations in a system and its variation with temperature can be quantified via the calculation of the structure factor:  $S(k, t) = \langle \psi_k(t) \psi_{-k}(t) \rangle$ ,  $\psi_k(t)$  being the Fourier transform of the order parameter [38]  $\psi(\vec{r}, t) (= \exp(i\theta(\vec{r})))$ ;  $\theta = 2\pi n/q$ ,  $n = 1, \dots, q$ . In the small  $k$  regime [ $\in (0, 0.4)$  or shorter], for the short-range cases,  $S(k, t)$  is described well by the Ornstein-Zernike relation [39, 40],  $S(k) = k_B T_s \chi / (1 + k^2 \xi^2)$ ,  $\chi$  being the susceptibility and  $\xi$  the correlation length. The average domain length,  $\ell(t)$ , of the clusters, during an

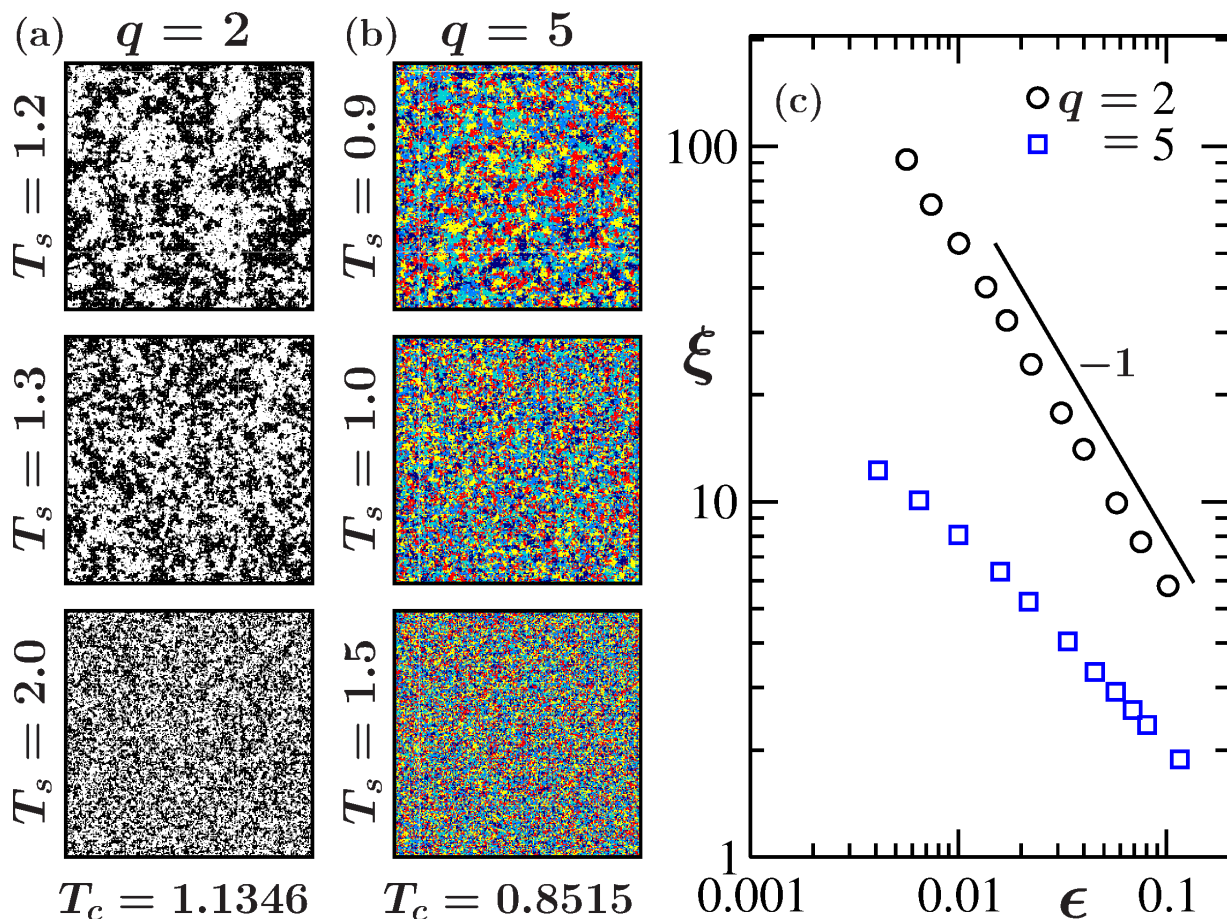


FIG. 1. Typical equilibrium configurations, for  $q = 2$  and 5 state Potts models, are shown in (a) and (b) from different starting temperatures  $T_s$  that are located above the respective critical temperatures  $T_c$ . (c) The plots of the correlation lengths,  $\xi$ , versus  $\epsilon$  ( $= (T_s - T_c)/T_c$ ), for the same Potts models. For  $q = 2$ ,  $\xi$  diverges as  $\epsilon^{-\nu}$ , with  $\nu = 1$  (see the solid line). These results are obtained for  $L = 256$ .

evolution towards the ferromagnetic state, has been estimated via the first moment of the domain size distribution function [41],  $P(\ell_d)$ , i.e.,  $\ell(t) = \int P(\ell_d, t) \ell_d d\ell_d$ , where  $\ell_d$  is the distance between two consecutive interfaces along a given direction.

### III. RESULTS

In Fig. 1 we depict how the choice of  $T_s$ , in the case of Potts model, can influence the structural features in the initial configurations, for different values of  $q$ . For both the considered cases, viz.,  $q = 2$  and 5, the configurations at higher  $T_s$  [see the snapshots at the bottom of the columns in (a) and (b)] appear random or structureless. With the decrease of  $T_s$ , spatial correlations emerge. This is more clearly identifiable in the case of  $q = 2$  for which one

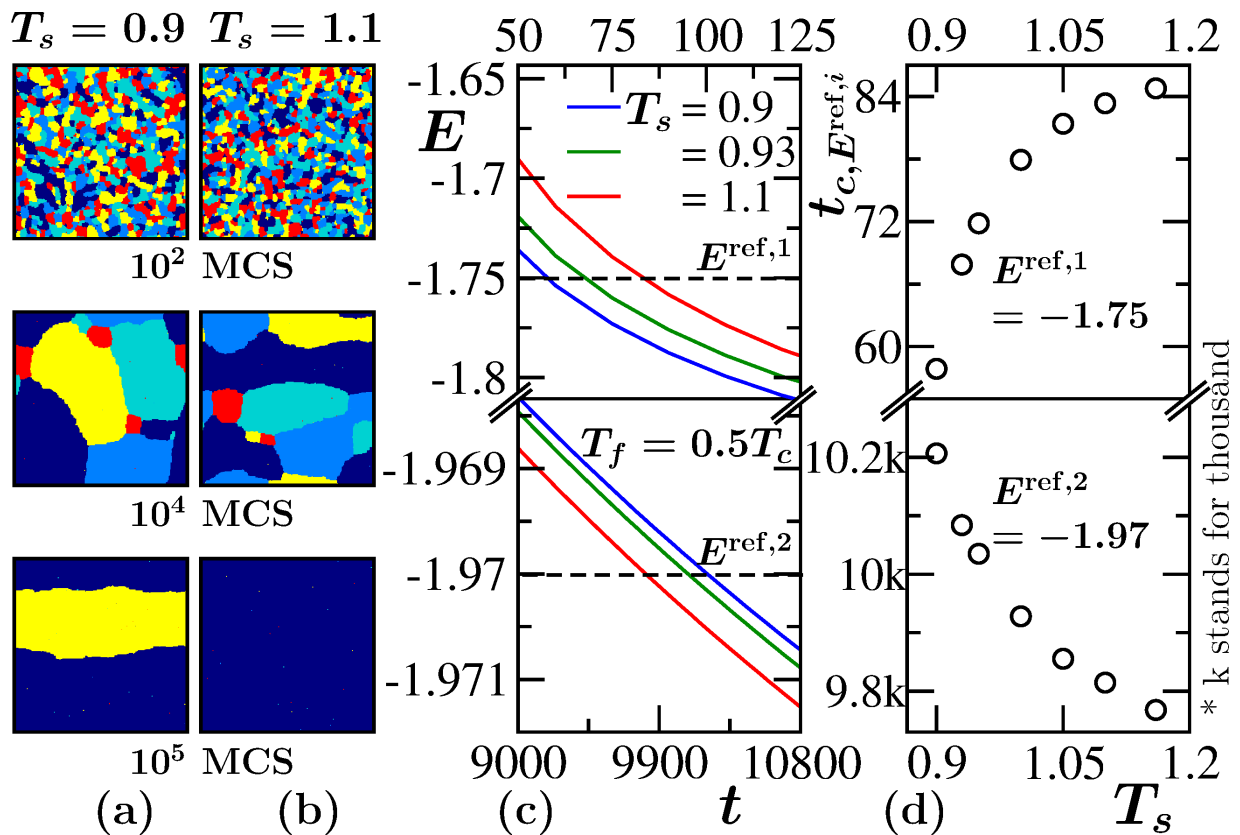


FIG. 2. Demonstration of relaxation in the 5-state Potts model, following quenches to  $T_f = 0.5 T_c$ , from different  $T_s$  values, with equal fraction of different spin states in boxes having  $L = 256$ . In (a) and (b) we show evolution snapshots, taken at different times, in units of standard Monte Carlo steps, for the systems initially at (a)  $T_s = 0.9$  and (b)  $T_s = 1.1$ . Different colours represent  $q$  different Potts states. (c) Plots of energy versus time, following quenches from several  $T_s$  values. The upper half corresponds to early time behavior and the lower one shows the late time behavior. The dashed horizontal lines are drawn to extract the times,  $t_{c, E^{\text{ref}, i}}$ ,  $i = 1, 2$ , corresponding to the crossings of certain values of energy  $E^{\text{ref}, i}$  by the energy curves of the systems with different  $T_s$ . (d) Plots of  $t_{c, E^{\text{ref}, 1}}$  (upper panel) and  $t_{c, E^{\text{ref}, 2}}$  (lower panel), versus  $T_s$ .

expects the critical divergence [39, 40]  $\xi \sim \epsilon^{-\nu}$ , with  $\nu = 1$ . For a wide range of  $\epsilon$  ( $= |T_s - T_c|/T_c$ ) such a behavior can be appreciated from Fig. 1(c). For  $q = 5$ , the phase transition is of first order [33], and we do not associate any exponent with the data set. The enhancement in the value of  $\xi$  can be appreciated for this  $q$  as well. In this case, the bending on the log-log scale over the whole presented range can well be, in addition to the finite-size effects, due to the first-order nature of the transition. Our expectation is that for this  $q$  the effect will be weaker. We proceed with the objective of quantifying it and to investigate if there exists any scaling rule [2] for arbitrary  $q$  that can as well comply with the other considered models.

We quench the systems from different [42]  $T_s$  to  $T_f = 0.5 T_c$ , for a large set of  $q$  values. In Fig. 2 we show results

obtained during evolutions following such quenches, for the 5-state Potts model. In parts (a) and (b) we show the snapshots at different stages of evolutions for  $T_s = 0.9$  and  $1.1$ , respectively. It is evident that the system from the higher  $T_s$  reaches the final equilibrium faster. This comparative picture is true not only for the chosen set of initial configurations, the observation indeed stands correct for a vast majority of the combinations of starting configurations. In part (c) we look at the decay of the average energy ( $E$ ) of the systems during the relaxation processes. We have included results for several  $T_s$ . Each of the data sets is presented after averaging over 300000 independent initial configurations. For clarity, we have enlarged the early and late time behavior separately, in the upper and lower panels, respectively. The orders of appearances of the plots, in terms of  $T_s$ , are systematic and opposite in the two panels. This implies that there are crossings amongst the energy curves, due to faster equilibrations of configurations prepared at higher  $T_s$ . This is the essence of Mpemba effect [1, 2, 18, 21]. For a demonstration of systematicity, we perform the following exercise. The dashed horizontal lines in these panels correspond to two reference energy values,  $E^{\text{ref},1}$  and  $E^{\text{ref},2}$ . We calculate the crossing time between a dashed line and the energy curve of the systems starting from each of the  $T_s$  values. Such a crossing time is denoted by  $t_{c,E^{\text{ref},i}}$ ,  $i = 1, 2$ . Part (d) of Fig. 2 shows  $t_{c,E^{\text{ref},i}}$  as a function of  $T_s$ . The upper and lower panels capture the early and late time behavior, respectively. The early time quantity, i.e.,  $t_{c,E^{\text{ref},1}}$ , increases with the increase in  $T_s$  but, at late times we see a different behavior, i.e.,  $t_{c,E^{\text{ref},2}}$  decreases with the increase in  $T_s$ . This implies faster relaxation of the systems with higher  $T_s$ , indicating the presence of ME.

The faster relaxation of the higher  $T_s$  systems can as well be quantified by calculating the average domain length,  $\ell(t)$ , a key probe to investigate coarsening dynamics [41–43]. In Fig. 3(a), we plot  $\ell(t)$ , vs  $t$ , for different  $T_s$  values, for  $q = 5$ . The early time behavior for different  $T_s$  are presented in the lower part of the divided graph. The late time comparisons are in the upper part. The systems starting at higher  $T_s$  tend to approach the new equilibrium earlier. This conveys a picture same as that derived from the energy decay, further strongly suggesting the presence of the Mpemba effect. We record the times at which the domain lengths of the systems at different finite  $T_s$  ( $< \infty$ ) values are crossed or overtaken by the corresponding plots for the systems starting from  $T_s = \infty$ . We denote this by  $t_{c,\ell_\infty}$ . In Fig. 3(b) we have plotted  $t_{c,\ell_\infty}$  as a function of  $T_s - T_c$ , for a few values of  $q$ , covering transitions of first as well as second order varieties. For each  $q$ , the crossing time increases with the approach of  $T_s$  to the corresponding  $T_c$ . Given that depending upon the value of  $q$  the nature of critical fluctuation is different, presence of any unique scaling behavior may not emerge from this figure. It appears, nevertheless, that for a given distance of  $T_s$  from  $T_c$ , the crossing time is longer for higher  $q$ . A quantitative picture for this is shown in Fig. 3(c). This is a signature that

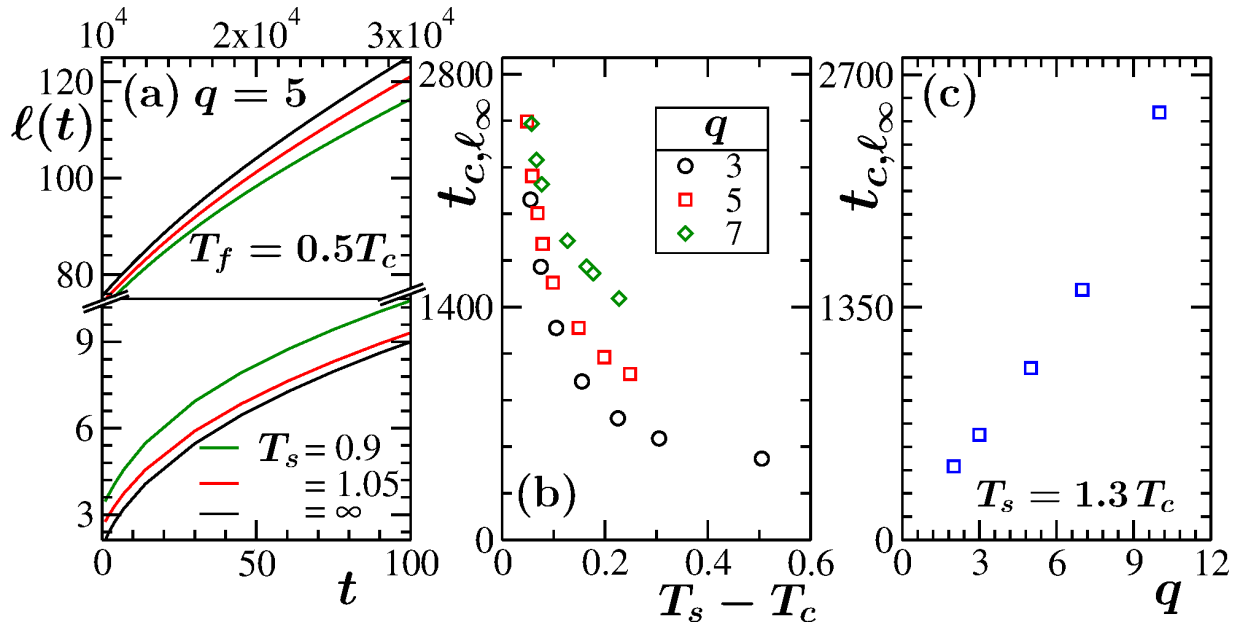


FIG. 3. (a) The plots of  $\ell(t)$  versus  $t$ , for the 5-state Potts model, for quenches from various  $T_s$  to  $T_f = 0.5 T_c$ . The lower frame captures the early time trend, while the upper frame depicts the late time behavior. (b) Plots of time,  $t_{c, \ell_\infty}$ , corresponding to crossing between growth curves for systems starting at  $T_s = \infty$  and a finite  $T_s$ , as a function of  $T_s - T_c$ , for different  $q$  values. (c) Plot of  $t_{c, \ell_\infty}$  versus  $q$  for systems prepared at  $T_s = 1.3 T_c$ . All results correspond to  $L = 256$ .

the ME gets weaker with the increase of  $q$ . Considering the influence of both  $q$  and  $T_s$ , the issue, however, is complex, that we address later.

Next we check whether the same scenario is true for the case of the LR Ising model. Due to the demanding computation, we analyze results for this case after averaging over 100 independent initial configurations. Note that the LR systems encounter finite-size effects much faster than its short-range counterpart, due to faster growth [34, 44, 45] with the decrease of  $\sigma$ . To avoid this problem, we choose big systems and a large value of  $\sigma$ , viz.,  $\sigma = 0.8$ , which, nevertheless, falls well within the long-range interaction domain [34]. In Fig. 4(a) we plot  $\ell(t)$ , vs  $t$ , for quenches to  $T_f = 0.3 T_c$ , from three  $T_s$  values, with  $L = 1024$ . From these plots it is clear that the systems with the highest  $T_s$  have the largest  $\ell(t)$ , at late times. Thus, ME appears to be present in the LR Ising model as well. Note that because of the above mentioned reasons we have used Ewald summation [35, 46], and parallelized our codes, in this case, to speed up the output.

So far we have dealt with 2D systems. Now we present results from the 3D NN Ising model in Fig. 4(b), where also the faster relaxation of the systems for the higher  $T_s$  value is quite clear. Here we have quenched the systems from different initial  $T_s$  values to  $T_f = 0.6 T_c$ . These results are presented after averaging over runs with 1440 independent

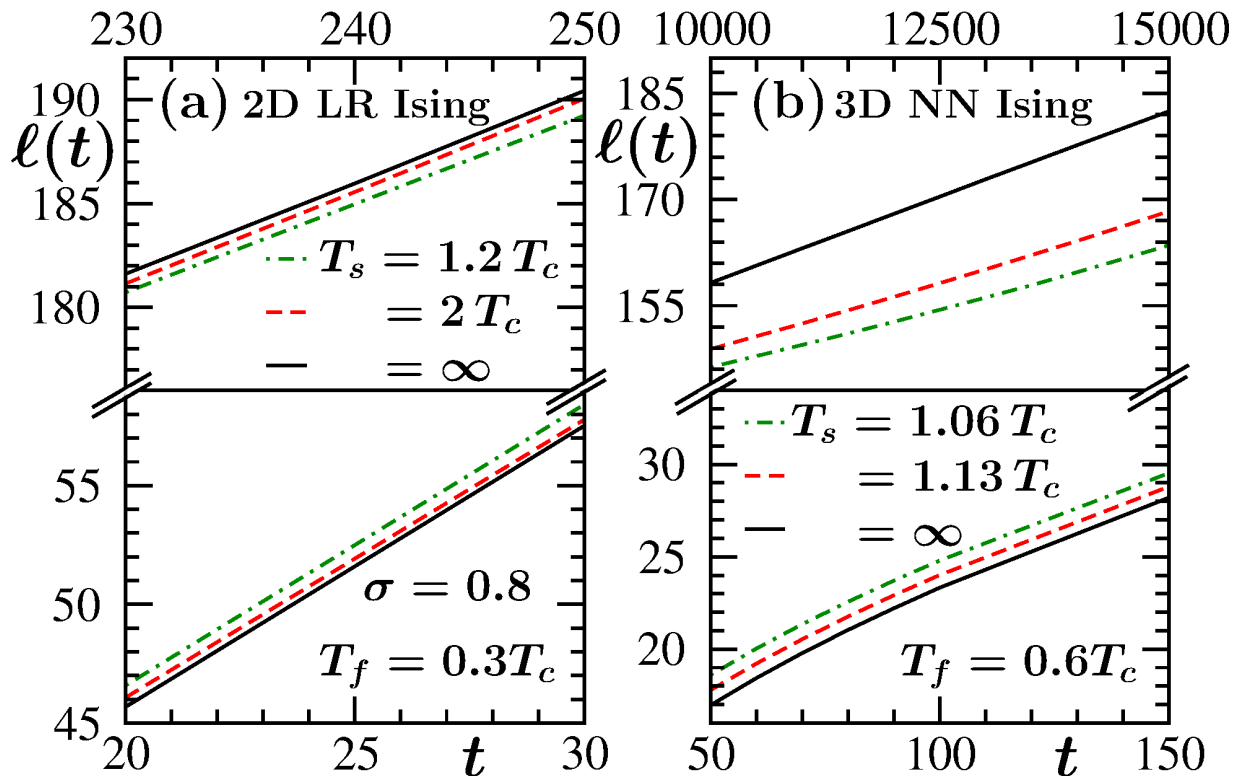


FIG. 4. (a) Plots of  $\ell(t)$  versus  $t$ , corresponding to a few different  $T_s$  values, for quenches to  $0.3T_c$ , for the LR Ising model. The value of  $\sigma$  is 0.8 and we have  $L = 1024$ . (b) Same as (a) but here the results are for the 3D nearest-neighbor (NN) Ising model with  $T_f = 0.6T_c$ , and  $L = 256$ .

initial configurations, with  $L = 256$ .

Returning to the Potts results in Fig. 3, we recall that an important objective of our work is to obtain a scaling picture [2]. Note that for different  $q$  values, one expects differing fluctuations in the critical vicinity. Thus, a unique behavior of the data sets in Fig. 3(b) should not be expected. It is more instructive to replace the abscissa variable there by  $\xi$ . Results from such an exercise is shown in Fig. 5(a). On a log-log scale it appears that the data sets from different  $q$  are reasonably parallel to each other. In Fig. 5(b), thus, we introduce a prefactor  $a$ , for the abscissa, constant for a particular value of  $q$ , to obtain an overlap of the data sets in Fig. 5(a). A nice collapse of the data sets can be appreciated. In fact, the results for the 2D and 3D Ising models also comply with that. It is worth mentioning here that accurate estimations of the crossing times require huge statistics.



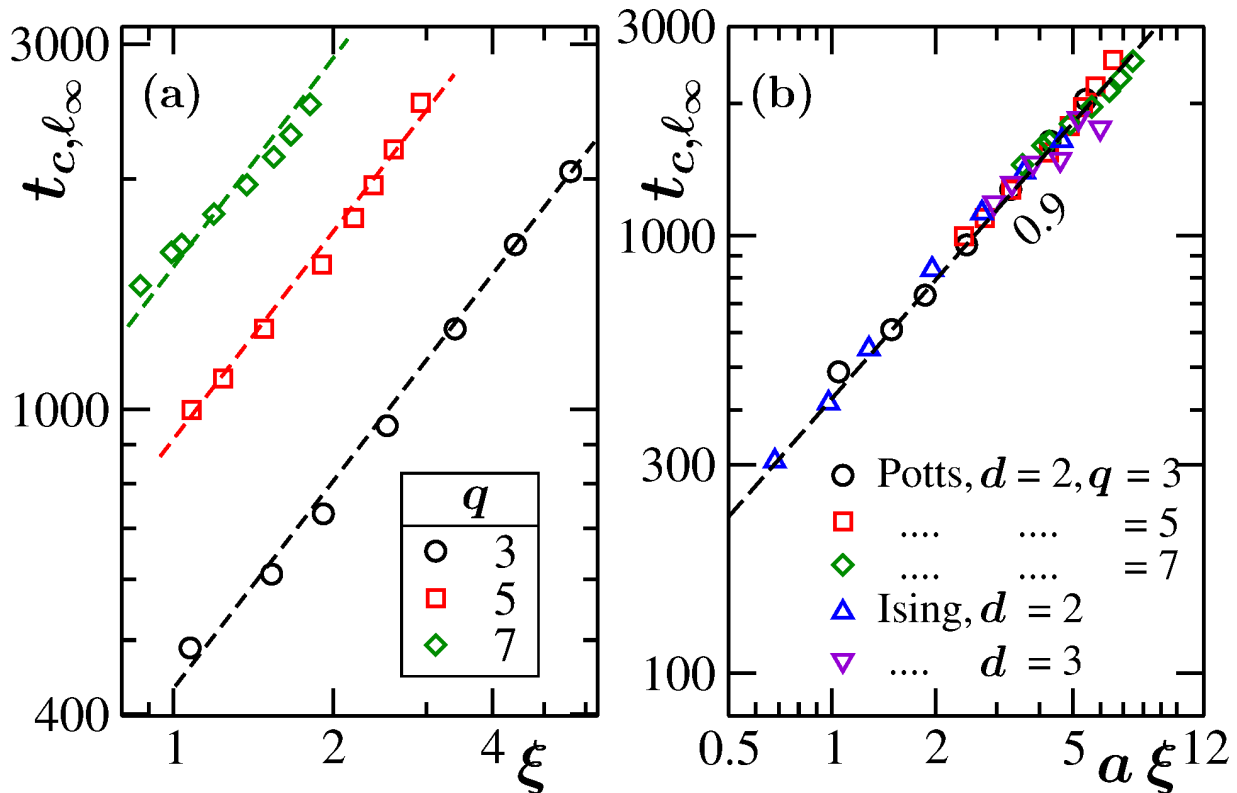


FIG. 5. (a) Plots of  $t_{c,l_{\infty}}$  versus  $\xi$ , for the Potts model, with a few different  $q$  values, on a double-log scale. (b) Same as (a) but here the abscissa of the data sets are scaled by constant factors to obtain a “possible” overlap. In addition to the results from the Potts cases ( $q \geq 3$ ), here we have included data for the NN Ising model, from different space dimensions. We expect discrepancy in scaling very close to  $T_c$  due to strong finite-size effects from multiple sources. Dashed lines represent power-laws.

#### IV. CONCLUSION

We have investigated the presence of the Mpemba effect [1–5] during para- to ferromagnetic transitions in several model systems with discrete spin values. These include short-range Ising model in  $d = 2$  and 3, as well as long-range Ising model in  $d = 2$ . Very extensive set of results are presented for the  $q$ -state Potts model for a wide range of  $q$  values. It is important to note that in none of the considered models there exist in-built frustration. Irrespective of the space dimension, range of interaction and order of transition, we have observed the Mpemba effect. It has interesting connection with the length of spatial correlations at the considered initial temperatures. The relative delay in approach to the final equilibrium, following quenches from para to ferro regions, with the lowering of starting temperatures, has unique dependence upon  $\xi$ . For second order transitions we have obtained a universal scaling for models with critical exponent  $\nu$  varying nearly by a factor of 1.6. More interestingly, the scaling is valid for

even first order transitions. This implies, for a given model, if two initial temperatures possess nearly same spatial correlations, possible for large  $q$ , configurations from these states will equilibrate almost simultaneously at the final temperature, showing no detectable ME, even for large differences in the  $T_s$ , in terms of times taken for reaching the final destination. We believe that our results contain important message for the understanding of the effect in water. Particularly the observation of it in the cases of first order transition can shed light on the mystery with respect to the latter. It will be interesting to investigate how the power-law dependence upon  $\xi$ , with exponent 0.9, may be connected to the scaling picture described in Ref. [2].

**Author contributions:** SKD proposed the topic, designed the problem, participated in the analyses, supervised the work and wrote the manuscript. NV oversaw a few coding details and took part in progress on all the models at the initial stages, alongside contributing to the writing. SC obtained all the final results on the Potts model, analyzed these, and contributed to the writing. SG and TP obtained and analyzed the results on the long-range and the 3D Ising models, respectively. Simulations of SKS provided the first hints of the Mpemba effect in the 3D Ising model.

**Acknowledgments:** SKD acknowledges a discussion with R. Pandit at an early stage and partial financial support from Science and Engineering Research Board, India, via Grant No. MTR/2019/001585. The authors are thankful to the supercomputing facility, PARAM Yukti, at JNCASR, under National Supercomputing Mission.

- 
- [1] E.B. Mpemba and D.G. Osborne, Cool?, *Physics Education* **4**, 172 (1969).
  - [2] S.K. Das, Perspectives on a Few Puzzles in Phase Transformations: When Should the Farthest Reach the Earliest?, *Langmuir* (2023).
  - [3] J Bechhoefer, A Kumar, R Chétrite, A Fresh Understanding of the Mpemba Effect, *Nat. Rev. Phys.* **3**, 534 (2021).
  - [4] D. Auerbach, Supercooling and the Mpemba Effect: When Hot Water Freezes Quicker Than Cold, *Am. J. Phys.* **63**, 882 (1995).
  - [5] M. Jeng, The Mpemba Effect: When Can Hot Water Freeze Faster Than Cold?, *Am. J. Phys.* **74**, 514 (2006).
  - [6] X. Zhang et al., Hydrogen-bond Memory and Water-skin Supersolidity Resolving the Mpemba Paradox, *Phys. Chem. Chem. Phys.* **16**, 22995 (2014).
  - [7] J. Jin and W.A. Goddard III, Mechanisms Underlying the Mpemba Effect in Water from Molecular Dynamics Simulations, *J. Phys. Chem. C* **119**, 2622 (2015).
  - [8] Y. Tao, W. Zou, J. Jia, W. Li, and D. Cremer, Different Ways of Hydrogen Bonding in Water - Why Does Warm Water Freeze Faster than Cold Water?, *J. Chem. Theory and Computation* **13**, 55 (2017).
  - [9] Z. Tang, W. Huang, Y. Zhang, Y. Liu, and L. Zhao, Direct Observation of the Mpemba Effect with Water: Probe the

Mysterious Heat Transfer, *InfoMat* **5**, e12352 (2022).

- [10] A. Kumar and J. Bechhoefer, Exponentially Faster Cooling in a Colloidal System, *Nature* **584**, 64 (2020).
- [11] Y.-H. Ahn, H. Kang, D.-Y. Koh, and H. Lee, Experimental Verifications of Mpemba-Like Behaviors of Clathrate Hydrates, *Korean J. Chem. Eng.* **33**, 1903 (2016).
- [12] P.A. Greaney, G. Lani, G. Cicero, and J.C. Grossman, Mpemba-Like Behavior in Carbon Nanotube Resonators, *Metall. Mater. Trans. A* **42**, 3907 (2011).
- [13] P. Chaddah, S. Dash, K. Kumar, and A. Banerjee, Overtaking While Approaching Equilibrium, arXiv.1011.3598 (2010).
- [14] A. Lasanta, F.V. Reyes, A. Prados, and A. Santos, When the Hotter Cools More Quickly: Mpemba Effect in Granular Fluids, *Phys. Rev. Lett.* **119**, 148001 (2017).
- [15] A. Torrente, M.A. López-Castaño, A. Lasanta, F.V. Reyes, A. Prados, and A. Santos, Large Mpemba-Like Effect in a Gas of Inelastic Rough Hard Spheres, *Phys. Rev. E* **99**, 060901(R) (2019).
- [16] A. Biswas, V.V. Prasad, O. Raz, and R. Rajesh, Mpemba Effect in Driven Granular Maxwell Gases, *Phys. Rev. E* **102**, 012906 (2020).
- [17] R. Gómez González and V. Garzó, Time-dependent homogeneous states of binary granular suspensions, *Physics of Fluids* **33**, 093315 (2021).
- [18] M. Baity-Jesi et al., The Mpemba Effect in Spin Glasses is a Persistent Memory Effect, *Proc. Natl. Acad. Sci. U. S. A.* **116**, 15350 (2019).
- [19] Z. Lu and O. Raz, Nonequilibrium Thermodynamics of the Markovian Mpemba Effect and its Inverse, *Proc. Natl. Acad. Sci. U. S. A.* **114**, 5083 (2017).
- [20] A. Gal and O. Raz, Precooling Strategy Allows Exponentially Faster Heating, *Phys. Rev. Lett.* **124**, 060602 (2020).
- [21] N. Vadakkayil and S.K. Das, Should a Hotter Paramagnet Transform Quicker To a Ferromagnet? Monte Carlo Simulation Results for Ising Model, *Phys. Chem. Chem. Phys.* **23**, 11186 (2021).
- [22] R. Holtzman and O. Raz, Landau theory for the Mpemba effect through phase transitions, *Commun Phys* **5**, 280 (2022).
- [23] A. Biswas, R. Rajesh, and A. Pal, Mpemba effect in a Langevin system: population statistics, metastability, and other exact results, *J. Chem. Phys.* **159**, 044120 (2023).
- [24] M.R. Walker and M. Vucelja, Anomalous thermal relaxation of Langevin particles in a piecewise-constant potential, *J. Stat. Mech.: Theory and Expt.*, 113105 (2021).
- [25] M. Vynnycky and S. Kimura, Can Natural Convection Alone Explain the Mpemba Effect?, *Int. J. Heat Mass Transf.* **80**, 243 (2015).
- [26] Z.Y. Yang and J.-X. Hou, Mpemba effect of a mean-field system: The phase transition time, *Phys. Rev. E* **105**, 014119 (2022).
- [27] F.J. Schwarzendahl and H. Löwen, Anomalous Cooling and Overcooling of Active Colloids, *Phys. Rev. Lett.* **129**, 138002

(2022).

- [28] Z. Cao, R. Bao, J. Zheng, and Z. Hou, Fast Functionalization with High Performance in the Autonomous Information Engine, *J. Phys. Chem. Lett.* **14**, 66 (2023).
- [29] S. Zhang and J.-X. Hou, Theoretical model for the Mpemba effect through the canonical first-order phase transition, *Phys. Rev E* **106**, 034131 (2022).
- [30] Aristotle, *Meteorologica*, translated by H.D.P. Lee (Harvard University Press, 1962), Book I, Chap. XII, pp. 85-87.
- [31] M. Matsumoto, S. Saito, and I. Ohmine, Molecular Dynamics Simulation of the Ice Nucleation and Growth Process Leading To Water Freezing, *Nature* **416**, 409 (2002).
- [32] D.P. Landau and K. Binder, *A Guide to Monte Carlo Simulations in Statistical Physics* (Cambridge University Press, Cambridge, 2009).
- [33] K. Binder, Static and dynamic critical phenomena of the two-dimensional  $q$ -state Potts model, *J. Stat. Phys.* **24**, 69 (1981).
- [34] A.J. Bray, Domain-growth Scaling in Systems with Long-range Interactions, *Phys. Rev. E* **47**, 3191 (1993).
- [35] T. Horita, H. Suwa, and S. Todo, Upper and Lower Critical Decay Exponents of Ising Ferromagnets with Long-range Interaction, *Phys. Rev. E* **95**, 012143 (2017).
- [36] U. Wolff, Collective Monte Carlo Updating for Spin Systems, *Phys. Rev. Lett.* **62**, 361 (1989).
- [37] K. Fukui and S. Todo, Order-N Cluster Monte Carlo Method for Spin Systems with Long-Range Interactions, *J. Comp. Phys.* **228**, 2629 (2009).
- [38] S. Puri, R. Ahluwalia, and A.J. Bray, Dynamical crossover in the clock model with a conserved order parameter, *Phys. Rev. E* **55**, 2345 (1997).
- [39] M.E. Fisher, The theory of equilibrium critical phenomena, *Rep. Prog. Phys.* **30**, 615 (1967).
- [40] H.E. Stanley, *Introduction to Phase Transitions and Critical Phenomena* (Clarendon Press, Oxford, 1971).
- [41] S. Majumder and S.K. Das, Diffusive domain coarsening: Early time dynamics and finite-size effects, *Phys. Rev. E* **84**, 021110 (2011).
- [42] S. Chakraborty, S.K. Das, Role of initial correlation in coarsening of a ferromagnet, *Eur. Phys. J. B* **88**, 1-9 (2015).
- [43] A.J. Bray, Theory of phase-ordering kinetics, *Adv. Phys.* **51**, 481 (2002).
- [44] H. Christiansen, S. Majumder, and W. Janke, Phase ordering kinetics of the long-range Ising model, *Phys. Rev. E* **99**, 011301(R) (2019).
- [45] S. Ghosh, S.K. Das, Aging During Phase Separation in Long-Range Ising Model, arXiv:2304.04996 (2023).
- [46] M.P. Allen and D.J. Tildesley, *Computer Simulation of Liquids* (Oxford University Press, 1991).